PHYSICAL REVIEW C VOLUME 23, NUMBER 1 JANUARY 1981

Phenomenology of continuum angular distributions. I. Systematics and parametrization

C. Kalbach
Triangle Universities Nuclear Laboratory, Duke University, Durham, North Carolina

F. M. Mann
Hanford Engineering Development Laboratory, Richland, Washington

(Received 20 June 1980)

A large number of experimental angular distributions have been studied for particles emitted into the continuum in preequilibrium nuclear reactions in order to study their systematics. For pure multistep direct reactions it has been found that to first order the shapes of these angular distributions are determined by the energy of the outgoing particle. In addition, there is evidence that the division of the cross section into multistep direct and multistep compound components with the latter having a symmetric angular distribution is a meaningful one. The shapes of the angular distributions can be described in terms of Legendre polynomials. The polynomial coefficients are given by simple phenomenological relations involving the energy of the outgoing particle. The same reduced coefficients are used for multistep direct and multistep compound processes except that only even order polynomials are considered in the latter case. The present formulation has been shown to have significant predictive ability for light ion reactions.

[NUCLEAR REACTIONS $A(a,b)$, $A = {}^{12}$C to ^{232}Th, $a = p, d, {}^{3}$He, ^{4}He, $b = n, p, d, t,$ ^{3}He, ^{4}He, $E = 18$–80 MeV, $E_b = 4$–60 MeV. Deduced systematics of $\sigma(E_b, \theta)/\sigma(E_b)$ in continuum. Parametrized $\sigma(E_b, \theta)/\sigma(E_b)$ in continuum with energy dependent Legendre polynomial coefficients.]

I. INTRODUCTION

For roughly the last ten years, the Griffin (or exciton) preequilibrium model for nuclear reactions has enjoyed significant success in reproducing a wide body of experimental data; both angle integrated energy spectra for emitted particles and excitation functions for forming specific product nuclides. What neither the Griffin model nor its near cousin, the hybrid model, has been able to do is to explain the angular distributions of the emitted particles. Among the preequilibrium models, initially only the intranuclear cascade (INC) model (a "refugee" from high energy physics) was able to calculate angular distributions. Its success level has been quite variable, and it is not readily adaptable to reactions involving complex particles.

Within the last several years, therefore, work has begun on extending preequilibrium calculations to include emitted particle angular distributions. A number of groups have approached the problem from quite different perspectives and assume different physical quantities to be important in determining the shapes of the distributions.

Several approaches involve modifying the existing exciton and hybrid models. The most thoroughly studied is due to Mantzouranis *et al.*[1,2] and has also been employed by Akkermans[3] and Machner.[4] It has been applied in both the exciton[1] and hybrid[2] formalisms. As in the INC model, free nucleon-nucleon scattering cross sections are used, but all of the angular information is assumed to be carried by a single fast particle degree of freedom. The dominant variable determining the shape of an angular distribution is the number of interactions made by the fast particle before emission. By contrast, all of the asymmetry in the angular distributions calculated by Plyuiko[5] is assumed to come from the single interaction or direct term. His approach is also more nearly related to the quantum mechanical compound nucleus model than to the INC. A J-dependent version of the Griffin model is derived, and the angular distribution is given in terms of Lengendre polynomials. Finally, in another J-dependent approach applicable in either the Griffin or hybrid model formalisms, Irie *et al.*[6] attribute the forward peaking in the angular distributions to a single surface l wave.

In addition, there are two approaches which are tied to direct reaction models. Tamura and Udagawa[7,8] assume a specific direct reaction mechanism and use a modified distorted-wave Born approximation (DWBA) formalism. Because of the complexity of the calculations, only one- and two-step processes are considered, and only a few emission energies across the spectrum are calculated. Intermediate energies are obtained by interpolation. The important physical quantities determining the shape of the angular distribution are hidden in the DWBA formalism. The other approach is due to Duisibaev *et al.*[9] and does not

claim to be quantitative. They attempt to reproduce data for (^{4}He,p), (^{4}He,d), and (^{4}He,t) reactions in terms of an evaporation component and a single direct stripping component treated by phase space methods. The shape of the angular distributions is determined primarily by the momentum of the transferred particle.

Finally, Feshbach *et al.*[10] have developed a complete quantum mechanical description for preequilibrium processes. It divides the cross section into two parts: statistical multistep direct (MSD) and statistical multistep compound (MSC). The MSD part has an unbound particle at each stage of the reaction and is expected to exhibit angular distributions which are peaked toward forward angles. The MSC part has all of the particles bound at each stage of the reaction and yields angular distributions which are symmetric about 90 degrees. Unfortunately, the calculations, particularly for the MSD part, are quite complex, and the theory has not been much compared with data. Even if it proves successful, it will be too complex for routine use in data analysis or in applied areas.

Thus, while many approaches have been proposed for calculating continuum angular distributions, all involve some serious approximations and/or computational complexities. Further, they disagree as to the physical quantities determining the shapes of the angular distributions. None has been shown to reproduce data under a sufficiently varied set of reaction conditions to be useful in applications requiring the prediction of many unmeasured angular distributions.

It was, therefore, decided to approach the problem phenomenologically, studying the systematics of a wide variety of experimental angular distributions and then finding a convenient (though not necessarily unique) way to parametrize them. While an effort has been made to be guided by physical principles, it can in no sense be claimed that the data have been "explained." Rather, the principal aim here was to provide a useful tool for people working in such applied areas as reactor shielding design and materials damage studies for fusion reactors. It is hoped, however, that the systematics observed in the data will also serve as a guide to theorists in the development of reaction models.

This work is described in a pair of papers. The present paper discusses the systematics observed in the data themselves and the parametrization used to describe them. A second paper,[11] hereafter referred to as II, discusses the modifications to the Griffin model required by this work.

Section II of this paper describes the general method used, and Sec. III describes the search for systematics in the data. These should be of special interest to theorists involved in trying to explain continuum angular distributions. The parametrization procedure is discussed in Secs. IV and V. Section IV describes "stage 1" or the choice of a mathematical form. "Stage 2," the setting of parameter values, is discussed in Sec. V. The predictive ability of the resulting parametrization has been tested against the full initial data set and some additional reaction systems. This is presented in Sec. VI.

II. THE METHOD

A. The data

In searching for systematics in the data it is important to have a highly varied set of reaction systems for study. The large collection of angular distributions assembled for preliminary investigation includes proton and complex particle projectiles, nucleon and complex particle ejectiles, target masses from 54 to 120, and incident energies from 18 to 62 MeV. The systems used[12-17] are listed above the dashed lines in Tables I and II.

In all such studies the limitations of the data must be seriously considered. One of the most serious of the problems encountered with measurements of continuum energy spectra is that of background subtraction. This is generally most severe at small forward angles, and in several instances data from the most forward angles were disregarded because of experimental problems. Even in other cases, it must be remembered that data from different laboratories might show slightly different apparent behavior due simply to different estimates of background contributions.

For the parametrization procedure, subsets of the initial data set have been used. These are indicated by entries in the columns labeled stage 1 and stage 2. The sytems[14,16,18] listed below the dashed lines in the tables are used here only to show the predictive ability of the parametrization derived.

B. Angular dependence assumed

It was decided at the outset to describe the angular distributions in terms of Legendre polynomials because we were confident of being able to obtain good fits to the data with a relatively small number of parameters, and the systematics of the data would be quantitatively displayed in the systematics of the Legendre polynomial coefficients.

Since existing models predict the magnitude of

TABLE I. Data for nucleon induced reactions.

Reaction	Projectile energy (MeV)	Ejectile energy (MeV)	No. of energies	No. of angles	Ref.	Stage 1	Stage 2
^{103}Rh(p,n)	18	5.5–12.5	4	10	12		a
^{107}Ag(p,n)	18	4.5–12.5	4	10	13		a
^{107}Ag(p,n)	25	6.5–18.5	5	16	13		a
^{54}Fe(p,p')	39	5–28	7	7	14		
^{54}Fe(p,p')	62	4–52	13	19	14	x	
^{120}Sn(p,p')	62	8–55	11	18	14	x	a,b
^{54}Fe(p,d)	39	7–16	4	7	14		
^{54}Fe(p,d)	62	5–35	7	21	14		
^{120}Sn(p,d)	62	8–42	10	20	14		
^{55}Fe(p,t)	39	10–12	2	7	14		
^{54}Fe(p,t)	62	10–35	6	21	14		
^{120}Sn(p,t)	62	8–42	8	20	14		
^{54}Fe$(p,{}^3$He$)$	62	14–33	6	21	14		
^{54}Fe$(p,{}^4$He$)$	39	8–24	5	7	14		
^{54}Fe$(p,{}^4$He$)$	62	10–48	10	21	14		
^{120}Sn$(p,{}^4$He$)$	62	12–55	10	20	14		
^{12}C(p,p')	62	30–40	2	18	14		
^{27}Al(p,p')	62	30–50	2	17	14		
^{54}Fe(p,p')	29	4–20	5	4	14		
^{197}Au(p,p')	29	20	1	4	14		
^{197}Au(p,p')	62	20–40	2	5	14		
^{209}Bi(p,p')	62	30–50	2	17	14		
^{54}Fe(p,d)	29	4–7	2	5	14		
^{12}C$(p,{}^4$He$)$	62	30	1	18	14		
^{27}Al$(p,{}^4$He$)$	62	30	1	17	14		
^{54}Fe$(p,{}^4$He$)$	29	8–20	4	5	14		
^{197}Au$(p,{}^4$He$)$	29	22	1	4	14		
^{197}Au$(p,{}^4$He$)$	62	25	1	6	14		
^{209}Bi$(p,{}^4$He$)$	62	20–40	2	18	14		

the cross sections, the present work centers on the shapes of the experimental angular distributions. These, in turn, are given not by the usual Legendre coefficients a_l, but by the reduced Legendre coefficients $b_l = a_l/a_0$, so that for the reaction (a,b)

$$\frac{d^2\sigma}{d\Omega\, d\epsilon}(a,b) = a_0(\text{tot}) \sum_{l=0}^{l_{\max}} b_l P_l(\cos\Theta) . \qquad (1)$$

In this work, then, the experimental b_l values have been searched for possible dependences on the major reaction parameters. The a_0 values are related to the single differential cross sections determined in preequilibrium reaction model codes by $a_0(\text{tot}) = (1/4\pi)(d\sigma/d\epsilon)$.

C. Multistep direct and multistep compound processes

Continuum angular distributions tend to be smoothly varying with angle, and the amount of forward peaking for a given reaction increases regularly with the energy of the outgoing particle.

Because of these qualitative similarities, it would seem that the detailed reaction mechanism should not play an important role. On the other hand, there must be some smooth way of going from the strongly forward peaked angular distributions generally characteristic of direct reactions to the nearly isotropic ones characteristic of compound nucleus reactions. Here the general ideas of MSD and MSC processes from Ref. 10 seem useful and have been adapted for use within the framework of the Griffin preequilibrium model as discussed in II. In addition to the two classes of reactions discussed in Ref. 10, a third class is encountered here in which the system has an unbound particle in some stages of the reaction and is totally bound in others. The cross sections for these processes have been included in the MSC components. The aim of the Griffin model calculations is simply to identify that part of the reaction cross section which might be expected to show forward peaked angular distributions.

In the case where the MSD/MSC distinction is a meaningful one, we assume that the two components will show the same systematics in the reduced polynomial coefficients, except that only the even order polynomials will contribute to the MSC

TABLE II. Data for complex particle induced reactions.

Reaction	Projectile energy (MeV)	Ejectile energy (MeV)	No. of energies	No. of angles	Ref.	Stage 1	Stage 2
^{63}Cu(d,p)	25	4.3–24.8	3	7	15		
^{63}Cu(d,d')	25	5.3–18.8	3	7–9	15		
^{63}Cu(d,t)	25	5.8–18.3	3	7–9	15		
^{63}Cu($d,^4$He)	25	10.3–27.8	3	8	15		
^{62}Ni(^{3}He,p)	24	4.3–24.8	3	7	15		
^{62}Ni(^{3}He,d)	24	5.3–18.8	3	7	15		
^{62}Ni(^{3}He,t)	24	5.8–11.3	2	7	15		
^{62}Ni(^{3}He,^{3}He′)	24	9.3–18.3	3	7	15		
^{62}Ni(^{3}He,^{4}He)	24	10.3–27.8	3	7	15		
^{54}Fe(^{4}He,p)	59	6–40	10	6	16		
^{59}Co(^{4}He,p)	42	10–32	5	8	17		*b*
^{61}Ni(^{4}He,p)	36	4.3–24.8	3	7	15		
^{103}Rh(^{4}He,p)	42	10–32	5	8	17		*b*
^{54}Fe(^{4}He,d)	59	6–33	8	6	16		
^{61}Ni(^{4}He,d)	36	5.3–18.8	3	7–8	15		
^{54}Fe(^{4}He,t)	59	8–31	5	6	16		
^{61}Ni(^{4}He,t)	36	5.8–18.3	3	7–8	15		
^{54}Fe(^{4}He,^{4}He′)	59	7–45	9	6	16		*b*
^{61}Ni(^{4}He,^{4}He′)	36	10.3–27.8	3	7	15		
^{27}Al(d,p)	80	60	1	7	18		
^{27}Al(d,d')	80	50	1	7	18		
^{58}Ni(d,d')	80	30	1	8	18		
^{208}Pb(d,d')	70	50	1	9	18		
^{232}Th(d,d')	70	40	1	8	18		
^{27}Al(d,t)	80	20	1	7	18		
^{58}Ni(d,t)	80	40	1	7	18		
^{90}Zr(d,t)	70	30	1	8	18		
^{232}Th(d,t)	70	40	1	8	18		
^{27}Al($d,^4$He)	80	40	1	7	18		
^{58}Ni($d,^4$He)	80	60	1	8	18		
^{90}Zr($d,^4$He)	70	50	1	8	18		
^{208}Pb($d,^4$He)	70	50	1	9	18		
^{12}C(^{4}He,p)	59	20	1	5	16		
^{12}C(^{4}He,^{4}He′)	59	20	1	5	18		

part. Thus the cross section of (1) becomes

$$\frac{d^2\sigma}{d\Omega\, d\epsilon}(a,b) = a_0(\mathrm{MSD}) \sum_{l=0}^{l_{\max}} b_l P_l(\cos\Theta) + a_0(\mathrm{MSC}) \sum_{\substack{l=0 \\ \Delta l=2}}^{l_{\max}} b_l P_l(\cos\Theta)\,. \qquad (2)$$

The various a_0 values are obviously related by $a_0(\mathrm{tot}) = a_0(\mathrm{MSD}) + a_0(\mathrm{MSC})$. The choice between (1) and (2) must be made based on comparisons with data.

Calculations were run with PRECO-D,[19] a modified version of the Griffin model computer code PRECO. To the MSD cross sections were added cross sections for direct nucleon transfer and for knockout and inelastic scattering processes involving complex particles.[20] At this time PRECO only calculates the energy spectra of the first particle emitted in a given reaction. Thus to the MSC cross sections were added evaporation components[21] for subsequent emission when these were needed and available.

III. SYSTEMATICS FROM LEGENDRE FITS

All of the experimental angular distributions above the dashed lines in Tables I and II were run through a Legendre polynomial fitting code and were analyzed using polynomials up through order 4. Polynomials of higher order were not included because of the small number of data points in some of the experimental distributions. Fits with the minimum reduced chi square consistent with statistically significant coefficients were chosen.

In examining the Legendre polynomial fits to the experimental angular distributions for systematics, attention was focused on those curves for

which the calculated percent of MSD was about 95% or greater so that the systematics of the reduced coefficients would be characteristic of MSD reactions. Angular distributions which contain both MSD and MSC contributions are considered more fully in the parametrization stage.

Figure 1 shows the reduced coefficients for the (p,p') and $(p,{}^4\mathrm{He})$ data. They are plotted vs the square root of the outgoing energy ϵ to make it easy to compare coefficients for either a given energy or a given momentum for the emitted particle. The figure demonstrates the following systematics in the regions where the cross section should be nearly pure MSD:

(1) The angular distributions are *not* sensitive to the incident energy. (39 and 62 MeV data are shown.)

(2) The angular distributions do *not* depend on target mass. ($A = 54$ and 120 data are shown.)

(3) Results for different outgoing particles agree when compared for the same outgoing energy ϵ (*not* momentum).

These conclusions are generally supported by the other proton induced reaction data even though the data for t and ^{3}He emission showed much more scatter in their b_l values due to the low cross section values.

The data for complex particle induced reactions also yielded reduced coefficients with lots of scatter. (See Fig. 2.) In this case it was due partly to the relatively small number of angles at which data were available. Within the uncertainty produced by this scatter, the first three observations are verified and a fourth is added:

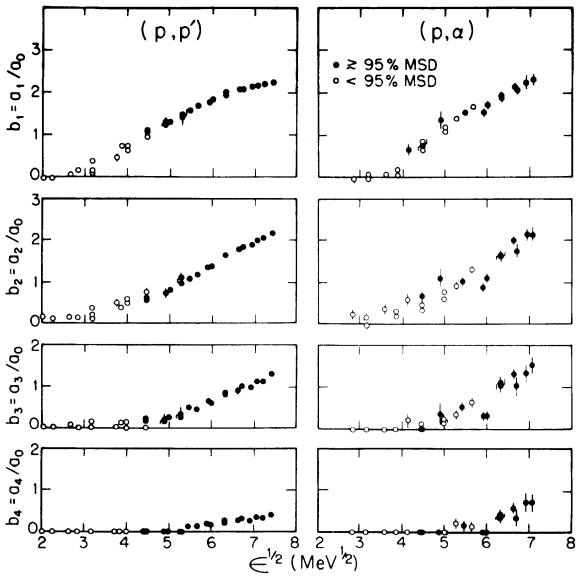

FIG. 1. Reduced Legendre coefficients from fitting individual angular distributions from proton induced reactions plotted as a function of the square root of the emission energy. Open (closed) points correspond to situations where the emission is calculated to be less (greater) than 95% MSD.

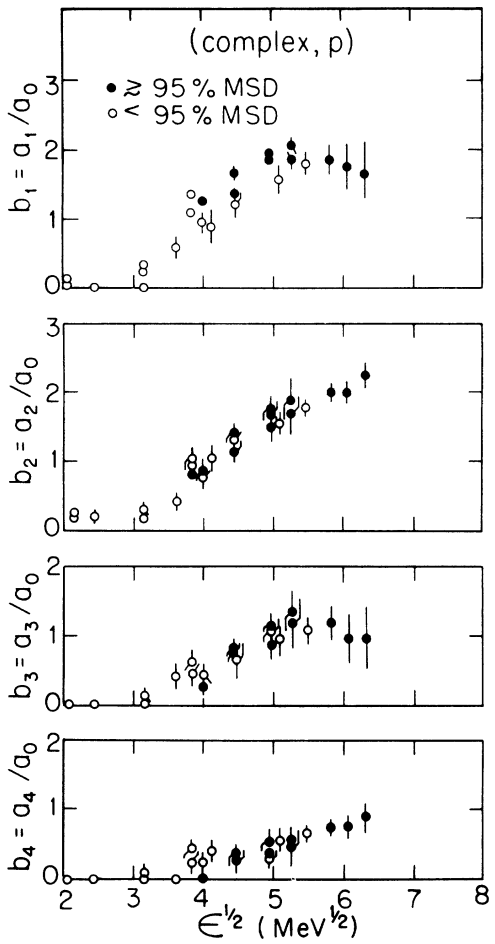

FIG. 2. Reduced Legendre coefficients from fitting individual angular distributions from complex particle induced reactions plotted as a function of the square root of the emission energy. Open and closed points have the same significance as in Fig. 1.

(4) There is a possible dependence of the shapes of the angular distributions on the nature of the projectile, with complex projectiles leading to more forward peaked curves.

The word "possible" is included as a qualifier because of the scatter of the results and because it seems strange to have a dependence on the nature of the projectile but not the ejectile. In addition, d, ^{3}He, and alpha projectile data seem to agree with one another.

Increased scatter in the b_l values for the (p,p') data is seen in Fig. 1 when both MSD and MSC

contributions are present. It is generally consistent with the idea that MSC contributions will be symmetric about 90 degrees and thus have no contribution from odd l. Further evidence for the importance of distinguishing between MSD and MSC processes is obtained by comparing the (p,n) coefficients with the (p,p') values shown in Fig. 1. The validity of the MSD/MSC division of the cross section is considered in more detail in Sec. IV.

IV. MATHEMATICAL FORM FOR THE b_l

A. Legendre fits

In Sec. III it was determined that the dominant reaction parameter governing the shapes of angular distributions for MSD reactions is the energy of the outgoing particle. Here the (p,p') data of Bertrand and Peelle[14] for an incident energy of 62 MeV are chosen for more detailed examination in an effort to find a way to parametrize the energy dependence. These data are indicated under stage 1 in Table I.

With data available at about 20 different angles in each distribution, a set of Legendre fits were performed allowing polynomials up through order 12. Due to the sparsity of data at back angles, it was necessary to add extra "data points" at angles of 150 and 170 degrees for $\epsilon \geq 40$ MeV. The errors assigned to these points were chosen to constrain the calculated cross sections from taking on unphysical values at back angles without otherwise seriously influencing the fits. The maximum order of the fits was varied from 2 to 12. Fits were chosen to have the minimum reduced chi square value consistent with having all of the b_l values statistically significant. In most cases l_{max} increased fairly smoothly with the outgoing energy. In the few cases where it did not, a fit one unit removed in l_{max} from the optimum was chosen. This usually resulted in only a small penalty in chi square. For the highest emission energy, terms up through P_8 were needed. The b_l values chosen are shown in Fig. 3.

B. Energy dependence of the b_l

An energy dependence for the reduced Legendre coefficients was sought that would be physically reasonable as well as able to account for the observed values.

In quantum mechanical theories of statistical reactions[5,22] when angular distributions for emitted particles are given in terms of Legendre polynomials, the polynomial coefficients are complicated combinations of angular momentum coupling factors, phase factors, and transmission coefficients. For this reason and because the observed

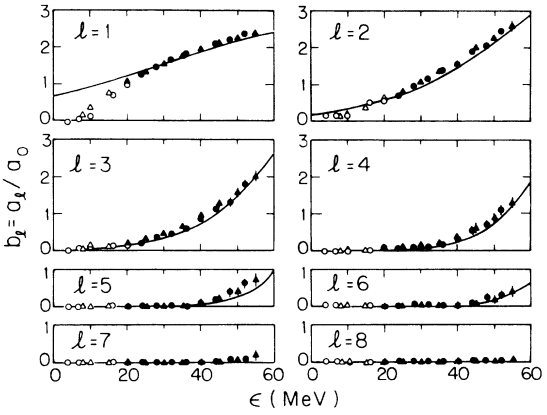

FIG. 3. Systematics of the reduced Legendre coefficients. The points result from fitting the 62 MeV (p,p') data with polynomials of order up through 12 assuming (1). Open (closed) points correspond to emission which is calculated to be less (more) than 98% MSD. The circles and triangles correspond to reactions on ^{54}Fe and ^{120}Sn, respectively. The curves show the systematics derived here and given by (3) and (5). For odd l they are directly comparable to the points only in the pure MSD limit.

b_l values are all positive and increasing with energy, an energy dependence similar to that of transmission coefficients was tried. By analogy to the weighted transmission coefficients for a parabolic barrier,[23] we have assumed that

$$b_l(\epsilon) = \frac{(2l+1)}{1+\exp[A_l(B_l-\epsilon)]}, \tag{3}$$

where A_l and B_l are free variables.

To study this dependence, we have considered initially only those angular distributions which are predicted to have 98% or more of their cross section due to MSD processes. This limit is somewhat tighter than the 95% used in determining the systematics. In this pure MSD limit, (1) and (2) become identical, and the systematics of the b_l's can be studied without having to know the importance of the distinction between MSD and MSC processes. By plotting $\ln\{[(2l+1)/b_l]-1\}$ vs ϵ for the 62 MeV (p,p') data and doing an approximate straight line fit, first estimates of A_l and B_l were obtained for $l = 1-5$.

C. Mixed MSD and MSC region

In the region where MSC cross sections contribute to the 62 MeV (p,p') cross section, no polynomials of order higher than 5 are needed to represent the data. Thus (3) and the approximate A_l and B_l values just determined are sufficient to allow a choice to be made between (1) and (2) as a way of treating mixed MSD and MSC cross sections. Calculations of the angular distributions

were therefore carried out using (2) with the ratio a_0 (MSD)/a_0(MSC) determined from PRECO-D and the sum a_0(MSD) + a_0(MSC) given by the empirical normalization a_0(tot) determined in the Legendre polynomial fitting. A second set of calculations was also carried out according to (1). The results are shown in Fig. 4. They indicate that the distinction between the two mechanisms is a meaningful one and that the assumption inherent in (2) for handling that distinction is adequate. Equation (2) has therefore been employed in the rest of this work.

It should be pointed out, however, that dividing the cross section into preequilibrium (including direct) and equilibrium parts would have worked almost as well as the MSD/MSC division.

D. Systematics of the A_l and B_l

The A_l and B_l values obtained in Sec. IV B above are, themselves, quite systematic, with A_l increasing and B_l decreasing as l decreases. These have been approximately fit with dependences of the type

$$A_l = k_1 + k_2[l(l+1)]^{m_1/2}, \tag{4a}$$

$$B_l = k_3 + k_4[l(l+1)]^{m_2/2}, \tag{4b}$$

where the m's are assumed to be integer variables and the k's are continuous variables. This type of dependence was chosen because it is simple and because the quantity $[l(l+1)]^{1/2}$ occurs naturally in quantum mechanical descriptions of angular momentum.

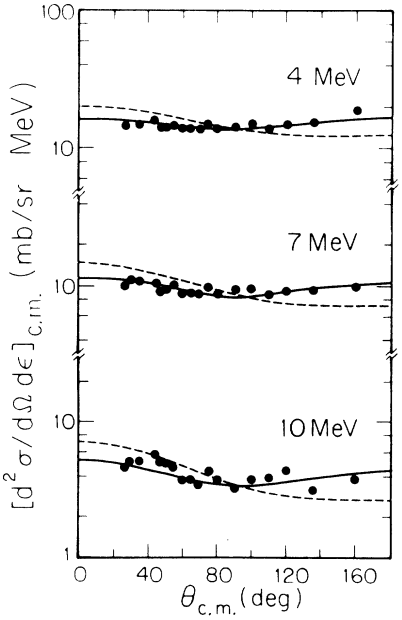

FIG. 4. Importance of distinguishing MSD and MSC processes. The points represent measured cross sections for the ^{54}Fe(p,p') reactions at 62 MeV incident energy and the indicated emission energy. The dashed curves are calculated as if all the cross section were MSD while the solid curves use (2) and the ratio of MSD to MSC cross sections predicted by the code PRECO-D.

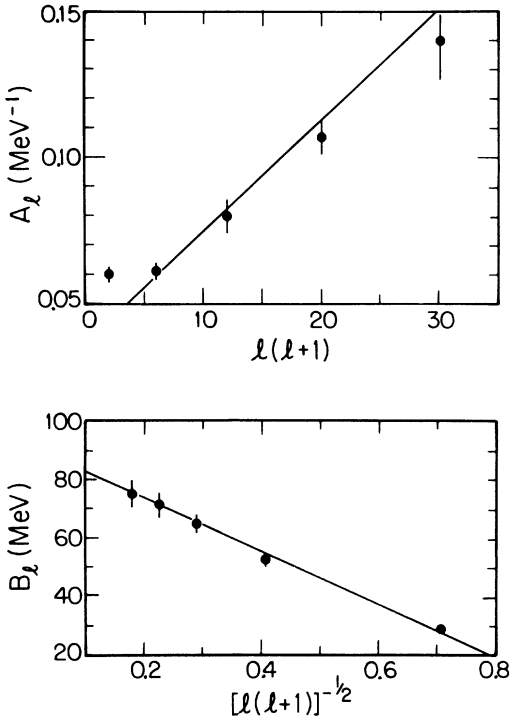

FIG. 5. Systematics of the A_l and B_l values. The points represent approximate values of these parameters derived from the fits to the 62 MeV (p, p') data displayed so as to show their possible l dependence. The straight lines are the result of least squares fitting to a subset of the full data. They are given by (5). The slope and intercept of each of the two lines were varied in the fitting process.

From graphical analyses, the quantity m_2 seems quite unambiguously to have the value −1. For m_1, values of 1, 2, or 3 seem possible. Plots of A_l vs $l(l+1)$ and B_l vs $[l(l+1)]^{-1/2}$ are shown in Fig. 5.

V. OPTIMUM PARAMETER VALUES

A nonlinear least squares fitting routine was used to optimize the various parameter values. Quantities varied for a given data subset were the four k values and the a_0(tot) = a_0(MSD) + a_0(MSC) for each spectrum. The ratio of the MSD to MSC cross section for each spectrum was held fixed at the value determined from PRECO-D. Preliminary studies indicated that reducing the maximum order of the polynomials from 8 to 6 did not significantly increase the reduced chi-square value, so only polynomials of order 0–6 are used in the remainder of this work.

A. Determination of m_1

The data set used in the determination of m_1 is indicated by an "a" under stage 2 in Table I. The motive for supplementing the 62 MeV (p,p') data is that large MSC contributions at low emission energies make these data fairly insensitive to the odd order Legendre coefficients. Lower bombarding energies provide the needed sensitivity. The (p,n) data were chosen in preference to the lower incident energy (p,p') data because of the larger number of angles represented in the angular distributions.

Fits to these data were carried out using m_1 values of 1, 2, and 3. The resulting reduced chi-square values were 3.7, 3.0, and 4.3, respectively. This clearly indicates that A_l varies linearly with $l(l+1)$, and this dependence has been adopted for the remainder of this work.

B. Determination of the k values

In order to arrive at the most universally useful set of values for the k parameters in (4), a different subset of the data was used containing a fairly even mixture of proton and alpha particle induced reactions. The data chosen are indicated by a "b" under stage 2 in Tables I and II. The (^{4}He,^{4}He′) data were chosen over the (^{4}He,p) data where it was available because the cross sections are higher (and therefore the statistics are better) at high emission energies. To give more even weighting to the proton and alpha projectiles without losing sensitivity to the high emission energies, the (p,p') data for emission energies below 45 MeV were reduced from 18 to 8 points per angular distribution, spaced fairly evenly in angle.

The fit with this data set gives a reduced chi-square of 5.3 and the dependences:

$$A_l = 0.036\ \text{MeV}^{-1} + 0.0039\ \text{MeV}^{-1}\, l(l+1), \quad (5a)$$

$$B_l = 92\ \text{MeV} - 90\ \text{MeV}\,[l(l+1)]^{-1/2}. \quad (5b)$$

These dependences are indicated on Fig. 5 along with the approximate values obtained from the 62 MeV (p,p') results.

The b_l values resulting from using (5) in (3) are shown in Fig. 3. It should be pointed out, however, that the points in the figure result from Legendre fits to the data assuming (1) while the parameters for the curves were determined using (2). Thus for odd l, only the solid points, corresponding to the pure MSD limit, should fall on the curves. The open points, corresponding to the mixed MSD and MSC domain, are expected to be a factor of $a_0(\text{MSD})/a_0(\text{tot})$ below the curves. For $l=1$ this seems to approximately verified while for $l=3,5,7$ the b_l values in the mixed region are too small for the effect to observed.

C. Uncertainties and limitations

One of the serious difficulties with using Legendre polynomials for fitting preequilibrium angular distributions is the very large forward-backward asymmetries encountered in the data at high emission energies. In some cases the cross section drops by 3 orders of magnitude. Thus, while the Legendre terms are adding at forward angles, there must be a nearly perfect cancellation at backward angles, and the back angle cross sections should be quite sensitive to the systematics of the Legendre coefficients.

To test this sensitivity, the angular distributions obtained from the results found above are compared with two other sets. In the first, the k values were determined with the a set used in Sec. V A, while in the second, the ^{120}Sn(p,p') data from the b data set in Sec. V B were replaced by the 62 MeV ^{54}Fe(p,p') data. Figure 6 shows the results of this comparison for a few typical cases. As expected, the calculated curves are quite stable at forward angles and at all angles for the low emission energies. What is, perhaps, more surprising is that exchanging the ^{120}Sn(p,p') for the ^{54}Fe(p,p') data in the subset used for fitting makes a more significant difference to the calculated angular distributions than exchanging the (^{4}He, ^{4}He′) and (^{4}He,p) for the (p,n) data. Figure 3 shows the extreme similarity of the reduced Legendre coefficients corresponding to the tin and iron data, yet small systematic differences in the data are apparently translated into significantly larger systematic differences in the calculated curves at back angles and high percent MSD once

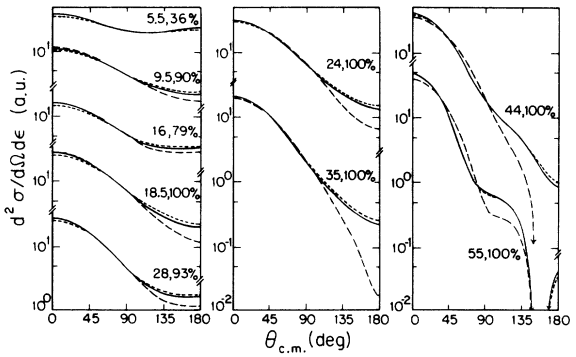

FIG. 6. Uncertainties in the parametrization derived. The curves represent angular distributions calculated for the indicated emission energy and percent MSD using the parameter values obtained in fitting three different subsets of the data. The solid curves are for the data indicated with a b under stage 2 in Tables I and II. The short dashed curves correspond to the data marked by an a under stage 2. The long dashed curves correspond to the replacement of the ^{120}Sn(p,p') data of the b set with the corresponding ^{54}Fe(p,p') data.

the added constraints of (3) and (4) are applied.

Thus the spread between the various classes of curves in Fig. 6 reflects the uncertainties in the systematics derived. These results indicate that the shape of the angular distributions are quite well determined at low emission energies and at low % MSD. As the degree of forward peaking in the angular distribution increases, the calculational uncertainty increases at backward angles and becomes quite significant for cross sections at the level of about 5% or less of the peak value.

VI. COMPARISONS WITH DATA

The usefulness of the empirical parametrization derived here should lie primarily in its ability to allow calculation of unmeasured angular distributions. To test its utility in this regard, comparisons of calculated angular distributions with three classes of data are presented:

(i) Data used in stage 2 of the fitting to determine the values of the m and k parameters.

(ii) Other data used in the original studies of Sec. III to determine the general systematics. (These are the remaining systems above the dashed lines in Tables I and II.)

(iii) Data not included in any of the analyses and used here to test the predictive ability of the systematics derived. (These are the systems listed below the dashed lines in the tables.)

The comparisons for groups (i), (ii), and (iii) are shown in Figs. 7, 8, and 9, respectively. The figures are weighted toward showing more examples at high emission energies because these are more difficult to reproduce. The normalizations of the calculated curves in these figures are chosen so as to facilitate comparisons between the shapes of the experimental and phenomenological angular distributions. They have no theoretical signifi-

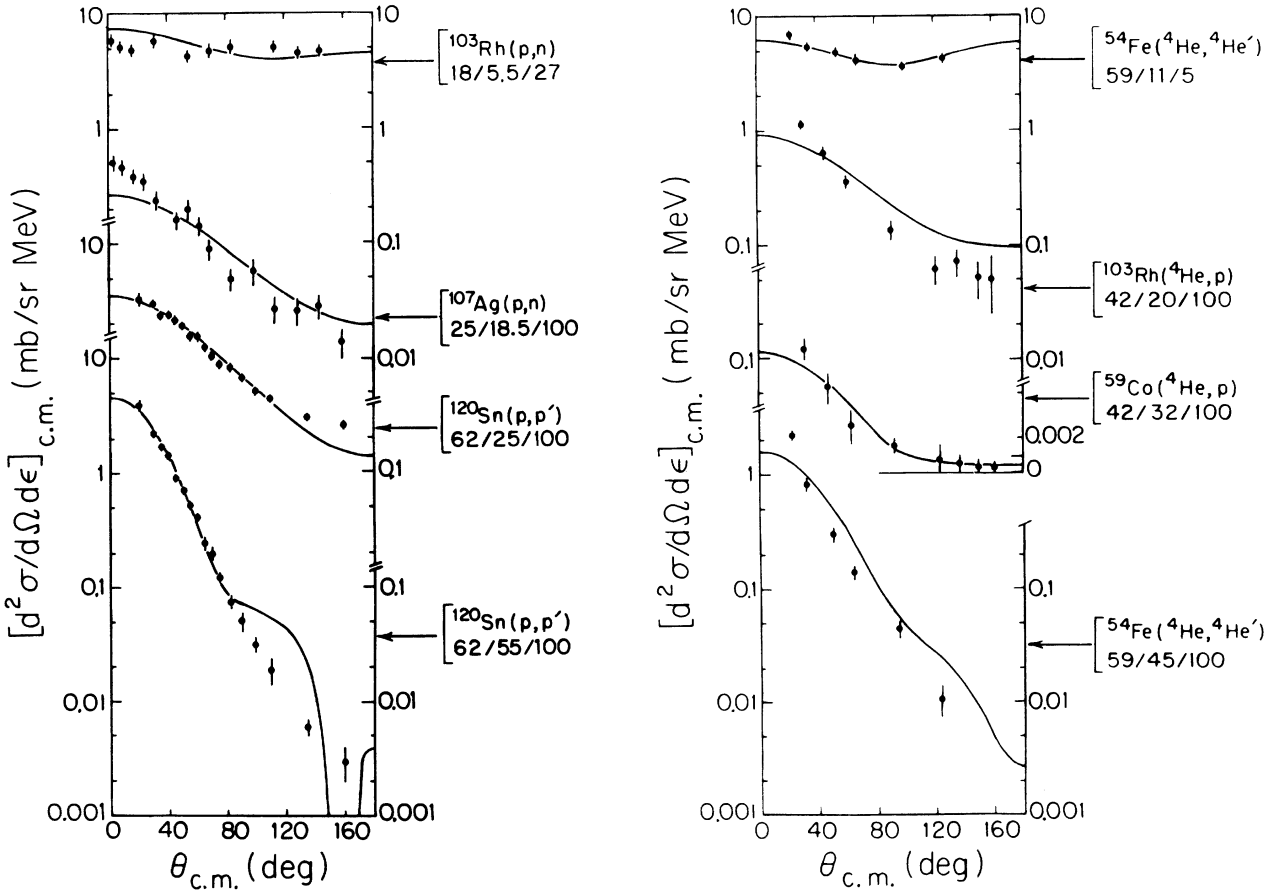

FIG. 7. Sample angular distributions for data systems used in stage 2 of the fitting procedure. The points show the data, while the curves are obtained using (2), (3), and (5). The three numbers beneath the reaction designations for each curve give the incident (lab) energy, the emission (c.m.) energy, both in MeV, and the % MSD. The plots are semilogarithmic. In a few cases where the uncertainties in the data points are as large as the cross sections themselves, a shift to a linear scale has been used at the bottom of the lowest decade.

cance. In practical applications the normalizations would be obtained from preequilibrium reaction model calculations. The agreement seen between calculation and experiment in the shapes of the angular distributions is quite good in most cases. Nor is there any significant difference between the three categories listed above as far as quality of agreement is concerned.

For proton induced reactions, good to very good agreement is found for (p,n), (p,p'), (p,d), $(p,{}^3\mathrm{He})$, and $(p,{}^4\mathrm{He})$ processes. For the (p,t) data, the quality of fit is slightly worse, with the calculations underestimating the degree of forward peaking found by experiment. The biggest systematic difficulty found for proton induced reactions is at emission energies of 50 to 55 MeV, where a shoulder develops at angles just past 90 degrees in the calculations but is not present in the data. The evidence of Fig. 6 suggests that these high emission energies are pushing the limit of applicability of the model.

For the complex particle induced reactions, the data of Ref. 15 at the higher emission energies show generally poorer agreement than the remaining systems. Comparing the $(d,{}^4\mathrm{He})$ and $({}^4\mathrm{He},p)$ data of Ref. 15 in Fig. 8 with the $(d,{}^4\mathrm{He})$ results in Fig. 9 and the 42 MeV incident $({}^4\mathrm{He},p)$ results in Fig. 7 implies that there may be a background

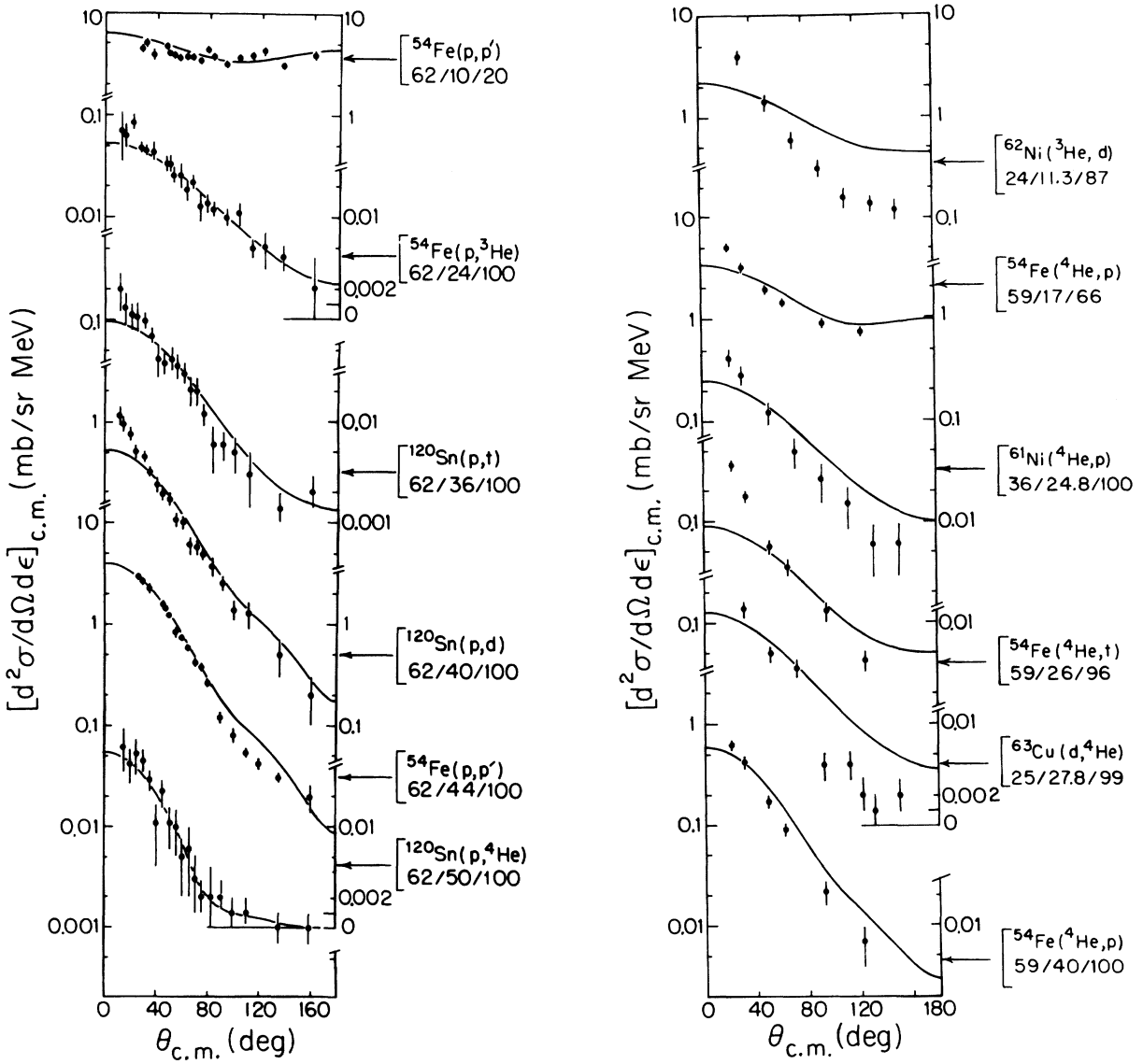

FIG. 8. Sample angular distributions for data systems in the original data set but not used in the parameter variation. Points and curves are as in Fig. 7.

subtraction problem in the Bonn data.[15] For the data from the other laboratories, the (^{4}He,p) and (^{4}He,^{4}He′) results again show good to very good agreement. For the (^{4}He,d) and (^{4}He,t) reactions, the agreement is quite good at low ϵ but deteriorates with increasing emission energy. For the deuteron induced reaction data of Ref. 18, the calculations agree about as well with the data as was the case for the (p,d) and (p,t) reactions, with the exception that very poor agreement is found for the ^{232}Th(d,d') results. What effect the occurrence of the ($d,d'f$) process would have is unknown, but certainly the (d,d') results for the lighter targets all show quite reasonable agreement between experiment and calculations.

The fact that the calculations agree about as well with the data from category (iii) as with the original data set suggests that the parametrization arrived at has significant predictive ability. This is particularly true since the target mass range in set (iii) is 12–232 as opposed to 54–120 in sets (i) and (ii).

The question of a possible projectile dependence for the Legendre coefficients seems to be answered in the negative. The comparable agreement between calculation and experiment found for proton and alpha particle projectiles points to the universality of the present prescription for light ion projectiles, as does the fact that the deuteron projectile data of Ref. 18 is fairly well reproduced.

VII. SUMMARY AND CONCLUSIONS

This work has demonstrated that the continuum angular distributions of particles emitted in the preequilibrium phase of a nuclear reaction follow extremely simple systematics. For emission energies where the cross section is almost totally multistep direct, the shape of the angular distribution is, to first order, determined exclusively by

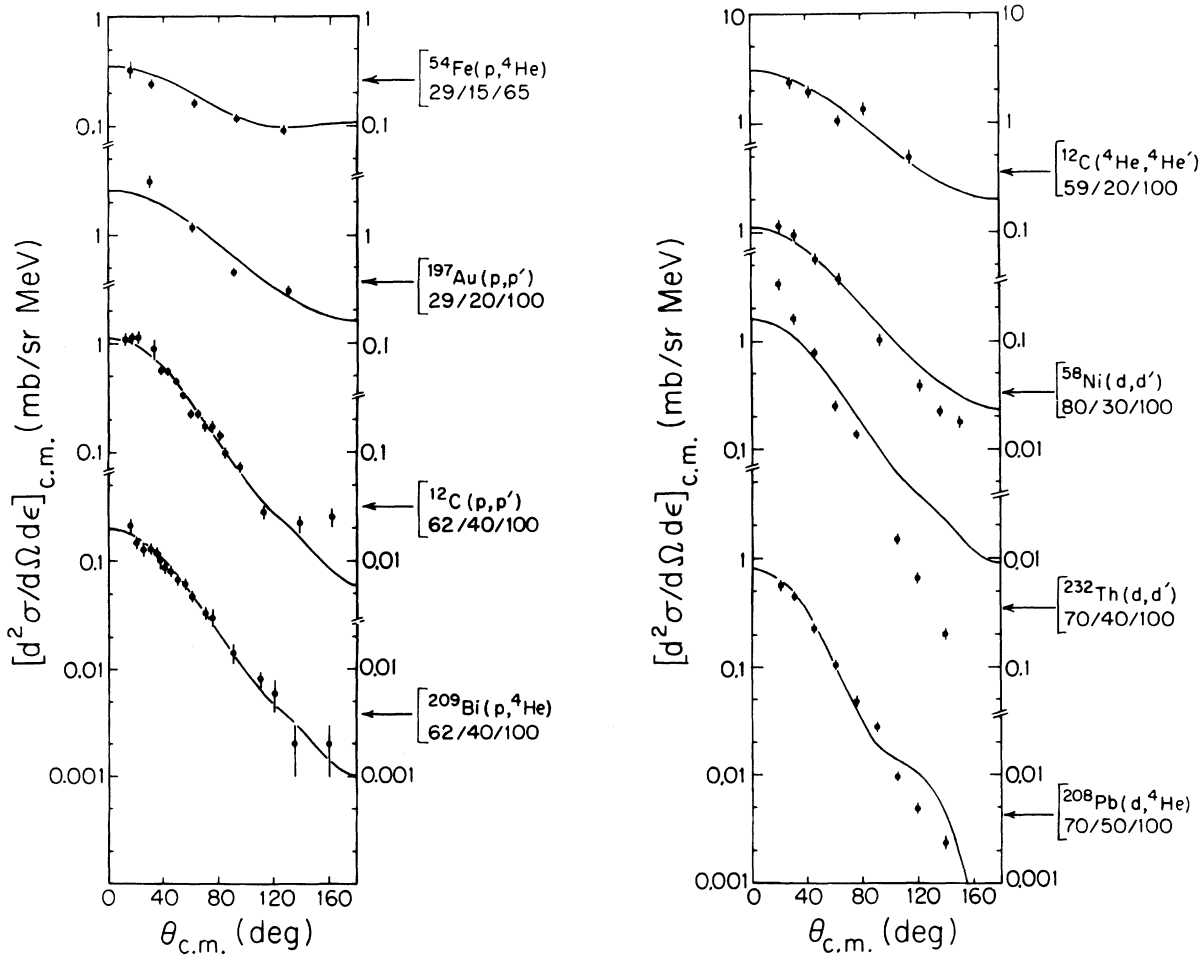

FIG. 9. Sample angular distributions for data systems not contained in the original data set. Points and curves are as in Fig. 7.

the emission energy.

A simple parametrization of the shapes of continuum angular distributions in terms of Legendre polynomials has been derived. The reduced Legendre coefficients are assumed to have the energy dependence of transmissions coefficients for a parabolic barrier, and are given in terms of two integral and four continuous parameters. The actual dependences are shown in (3) and (5). For emission energies where both multistep direct and multistep compound mechanisms have significant contributions, the same reduced coefficients are used, but only the even order polynomials are considered in describing the MSC contribution.

While the semiempirical parametrization derived here is certainly not unique, it has been shown to have considerable predictive ability. This makes it now possible to obtain reasonable estimates of unmeasured angular distributions by combining these results with existing models for calculating preequilibrium reaction cross sections.

The present systematics, while quite general, seems to do best at explaining continuum data for reactions where only nucleons and alpha particles are involved. For reactions involving mass 2 and mass 3 particles, the degree of forward angle peaking in the data is sometimes slightly underestimated. The systematics seems to work for targets ranging from mass 12 up to mass 200 and for bombarding energies of from 18 MeV up to at least 80 MeV. It does well for emission energies ranging from the evaporation peak at just a few MeV up to about 40 or 45 MeV. For emission energies of 50 to 60 MeV it does well only at forward angles, and the method of Legendre polynomials has difficulty reproducing the back angle cross sections which are of the order of a few percent or less of the peak cross section. In most practical applications this should not be very important. At still higher emission energies, a different mathematical form for the angular distributions would seem to be needed.

The observed simple dependence of the shape of the angular distributions on only the emission energy and the fraction of the cross section which is MSD is not accounted for in the theoretical approaches so far proposed, or is at least not obvious in their formalisms. It thus provides a useful indication of what simple reaction models should be trying to explain.

In summary, it is felt that this work has given experimentalists and people in applied areas a useful way to calculate unmeasured continuum angular distributions for light ion reactions. In addition, it has provided guidance for theorists working to obtain more rigorous descriptions of angular distributions within the context of preequilibrium reaction models.

ACKNOWLEDGMENTS

This work was supported by Hanford Engineering Development Laboratory. HEDL is operated by Westinghouse Hanford Company, a subsidiary of Westinghouse Electric Corporation, under DOE Contract No. DE-AC-76FF02170. One of the authors (C.K.) would like to acknowledge the hospitality of the Triangle Universities Nuclear Laboratory.

[1]G. Mantzouranis, H. A. Weidenmueller, and D. Agassi, Z. Phys. A 276, 145 (1976).
[2]G. Mantzouranis, Phys. Rev. C. 14, 2018 (1976).
[3]J. M. Akkermans, Phys. Lett. 82B, 20 (1979).
[4]H. Machner, Phys. Lett. 86B, 129 (1979).
[5]V. A. Plyuiko, Yad. Fiz. 27, 1175 (1978) [Sov. J. Nucl. Phys. 27, 623 (1978)].
[6]Y. Irie, M. Hyakutake, M. Matoba, and M. Sonoda, Phys. Lett. 62B, 9 (1976).
[7]T. Tamura, T. Udagawa, D. H. Feng, and K.-K. Kan, Phys. Lett. 66B, 109 (1977).
[8]T. Tamura and T. Udagawa, Phys. Lett. 71B, 273 (1977).
[9]A. D. Duisebaev, V. I. Kanashevich, E. M. Saprykin, I. B. Teplov, D. A. Shalbaev, and N. P. Yudin, Yad. Fiz. 27, 1156 (1978) [Sov. J. Nucl. Phys. 27, 613 (1978)].
[10]H. Feshbach, A. Kerman, and S. Koonin, Ann. Phys. (N.Y.) 125, 429 (1980).
[11]C. Kalbach and F. M. Mann, following paper, Phys. Rev. C 23, 124 (1981).
[12]C. Kalbach, S. M. Grimes, and C. Wong, Z. Phys. A 275; 175 (1975).
[13]S. M. Grimes, J. D. Anderson, and C. Wong, Phys. Rev. C 13, 2224 (1976).
[14]F. E. Bertrand and R. W. Peelle, Phys. Rev. C 8, 1045 (1973).
[15]J. Bisplinghoff, J. Ernst, R. Lohr, T. Mayer-Kuckuk, and P. Meyer, Nucl. Phys. A269, 147 (1976).
[16]F. E. Bertrand, R. W. Peelle, and C. Kalbach-Cline, Phys. Rev. C 10, 1028 (1974).
[17]R. W. West, Phys. Rev. 141, 1033 (1966).
[18]J. R. Wu, C. C. Chang, and H. D. Holmgren, Phys. Rev. C 19, 370 (1979).
[19]C. Kalbach, informal report (PRECO-D) available from author.
[20]C. Kalbach, Z. Phys. A 283, 401 (1977).
[21]C. K. Cline and M. Blann, Nucl. Phys. A172, 225 (1971).
[22]H. Feshbach, *Nuclear Spectroscopy B*, edited by Fay Ajzenberg-Selove (Academic, New York, 1960), p. 625.
[23]D. L. Hill and J. A. Wheeler, Phys. Rev. 89, 1102 (1953).